Michael Petrides and Scott Mackey

Quantitative demonstration of comparable architectonic areas within the ventromedial and lateral orbital cortex in the human and the macaque monkey brains

Published in:

European Journal of Neuroscience 2010 Dec. 32(11)1940-50. Epub 2010 Nov 3.

doi: 10.1111/j.1460-9568.2010.07465.x
http://onlinelibrary.wiley.com/journal/10.1111/(ISSN)1460-9568

Quantitative Demonstration of Comparable Architectonic Areas within the Ventromedial and Lateral Orbital Frontal Cortex in the Human and the Macaque Monkey Brain

Abbreviated title: Comparable Cortical Areas in Human and Macaque

Scott Mackey [1,2] and Michael Petrides [1]

1. Cognitive Neuroscience Unit, Montreal Neurological Institute, McGill University, 3801 University Street, Montreal, Quebec, H3A 2B4, Canada

2. Brain Research Center, University of British Columbia, 2211 Wesbrook Mall, Vancouver, British Columbia, V6T 2B5, Canada

Corresponding Author:
Scott Mackey
Brain Research Center
University of British Columbia
2211 Wesbrook Mall
Vancouver, British Columbia
V6T 2B5, Canada

tel: (604) 822-1770
fax: (604) 822-7866
e-mail: mackeys@interchange.ubc.ca

Number of Figures: 8
Number of Tables: 3

Keywords: Density Profiles, Cortical Architecture, Ventromedial Frontal Cortex, Orbitofrontal Cortex

Funded by the Canadian Institutes of Health Research

#MOP-14620 to Michael Petrides

1. Abstract

The orbital and ventromedial frontal cortical regions of the human and the macaque brains are composed of several spatially discrete areas which are defined histologically by their distinctive laminar architecture. While considerable information has been collected on the function and anatomical connections of specific architectonic areas within the orbital and ventromedial frontal cortex of the macaque monkey, the exact location of comparable areas in the human brain remains controversial because, until now, interspecies comparisons have relied upon imprecise qualitative descriptions of the cortical architecture. We resolved this problem by quantifying the areal densities of cortical layers IV and Va in a large sample of the orbital and ventromedial frontal cortex in both species. We present here the first quantitative demonstration of architectonically comparable cortical areas in the human and the macaque brains. Further, we found that the quantified architectonic features arrange areas within the orbital and ventromedial frontal cortex along two dimensions: an anterior-to-posterior and a medial-to-lateral dimension. On the basis of these findings, and in light of known anatomical connections in the macaque, we suggest that this region of the human cortex contains at least two hierarchically structured networks of areas.

2. Introduction

Human orbital and ventromedial frontal cortex dysfunction has been implicated in a spectrum of emotion-related psychiatric syndromes including mood disorders, addiction, schizophrenia and psychopathy (Ressler & Mayberg, 2007; Everitt *et al.* 2007; Blair, 2004; Goldstein *et al.*, 1999). Damage to the human orbital and adjacent ventromedial frontal cortex (Fig. 1) has long been associated with emotional deficits that, if as yet incompletely understood, have devastating real-life consequences in terms of the patients' interpersonal, occupational and financial behavior (Harlow, 1848/1999; Damasio, 1996). New research, combining clinical and neuroimaging data obtained on the human brain with the results of experimental techniques in the macaque monkey which are not possible in human subjects, has focused on articulating the contribution of individual architectonic cortical areas to specific emotion related processes (Murray, O'Doherty & Schoenbaum 2007; Kringelback & Rolls, 2004; Phelps *et al.* 2004). The success of this effort hinges on the ability of researchers to identify accurately comparable areas across species. For example, it has been reported recently that deep brain stimulation of the posterior ventromedial cortex (Fig. 1) has positive therapeutic effects in a patient population suffering from pharmacologically intractable depression (Ressler & Mayberg, 2007). The cortical region targeted by stimulation contains several architectonically distinct areas and it is unknown which areas are critical to the effects of the treatment or how they operate. If comparable architectonic areas between the human and the macaque brains were well defined, significant improvement in the design of this procedure (e.g. the placement of electrodes within specific components of the region of interest) and the theoretical rationale behind it could be obtained by studying the effects of precise lesions and recording the electrophysiological activity of relevant neuronal populations in the monkey.

Minimally, comparable areas should i) exhibit a common set of distinctive architectonic features (Fig. 2B), and ii) occupy the same position within a fixed constellation of surrounding areas in both species. The controversy over the location of comparable areas in the human and the macaque brains results from a disagreement about the qualitative terms which describe the architectonic features that define areas and which have been interpreted inconsistently by different investigators in the human brain. Although the qualitative terms *agranular, dysgranular* and *granular*, which describe observable degrees of granule cell density in layer IV, have conventionally established meanings in the monkey (Walker, 1940; Barbas & Pandya, 1989; Morecraft, Geula & Mesulam, 1992; Carmichael & Price 1994; Petrides & Pandya, 1994 Cavada *et al.,* 2000; Dombrowksi and Barbas, 2001), such that the central posterior part of the monkey orbital frontal cortex, area 13, is recognized by consensus as dysgranular, the cortex on the human posterior orbital gyrus (Fig. 1), for example, has been alternately and incompatibly described as agranular (Hof, Mufson & Morrison, 1995; Beck, 1949) dysgranular (Petrides & Mackey, 2005) and granular (Ongur, Ferry & Price, 2003). Moreover, since dysgranular monkey area 13 should correspond according to criterion (i) above to a dysgranular cortical area in the human, the implied location of a comparable human area 13 as illustrated in Figure 2A differs substantially between investigators (Petrides & Mackey, 2005; Hof, Mufson & Morrison 1995; Ongur, Ferry &

Price, 2003; Semedeferi *et al.,* 1998; Beck, 1949) lying in some instances several centimeters apart. In the present study, we remove the inherent uncertainty of interspecies comparisons made on qualitative descriptions by quantifying the architectonic features of interest over a large region of the human and the macaque brains.

3. Materials and Methods

3.1 Summary

In brief, quantitative sampling according to the method described by Mackey & Petrides (2009) was performed on histologically prepared sections obtained from 16 human hemispheres and seven monkey hemispheres. The series of sections (194 human and 46 macaque sections) selected for sampling represented equally all architectonic areas within the ventromedial and orbital surfaces of the frontal lobe but were otherwise chosen at random. On digital images of the sections, cells were segregated according to their size into one of two density images per histological section: a granule cell density image and a pyramidal cell density image (Fig 3B, C). The cortical ribbon contained in the density images was sampled from layer II to the white matter along equally spaced transverse lines (Fig. 3D). The sample along any one transverse represents a *profile* of the neuronal density at that cortical location (Mackey & Petrides, 2009). Transverse sampling assumes that density profiles sampled from one architectonic area share a common set of features which distinguish them from profiles sampled from spatially adjacent architectonic areas. On the density profiles, we calculated the mean density of specific cortical layers which had been manually identified on a separate identically sized set of images (Fig.4, 5)

3.2 Histology

The use of monkey and human specimens in this study was approved by, respectively, the McGill University Animal Care Committee in accordance with the Canadian Council for Animal Care guidelines and the McGill University Ethics Committee. One human brain was embedded in celloidin and sectioned coronally at a thickness of 36µm. The remaining 12 hemispheres were blocked, embedded in paraffin and sectioned at a thickness of 12µm. The macaque hemispheres were flash frozen in an isopentane bath and sectioned at 35µm. Three macaque hemispheres were cut in the coronal plane and two hemispheres each in the sagittal and horizontal planes. A one-in-ten series of sections from each hemisphere were mounted on glass microscope slides and prepared histologically with a Nissl cell body stain.

3.3 Imaging and Preprocessing

Imaging and sampling was coordinated by software designed for computer microscopy (Northern Eclipse, Empix). Digital images of the histological sections were acquired under low power magnification (10 x 1.00) (DMR-XA2, Leica). From each imaged histological section seven equally sized images representing different aspects of the cortical lamina were derived for sampling (Fig. 3A-C, 4C-F). The first five sampling images indicated the locations, respectively, of layers II, IV, Va, and VIa as well as the outer contour (the boundary between layers I and II) and inner contour (the boundary between layer VI and the underlying white matter) of the cortex. The locations and contours were traced manually on the original images of the histological sections (Fig. 4A-F). In areas 24 and 25, where layer IV is absent, the boundary between layers III and V was used instead of IV. The remaining three sampling images contained differential information on the cell density of the cortical layers: granule, pyramidal and general (both granule and pyramidal) cell density (Fig. 3A-C). To construct the granule and pyramidal cell density images thresholded cell bodies were classified on the basis of their size by a spatial binning algorithm. The parameters of one bin were adjusted to collect cells within the size range of typical of granule cells. Larger cells were classified as pyramidal. To stabilize the sample, the granule, pyramidal and general cell density images were convolved with a Gaussian blurring kernel.

3.4 Sampling and Analysis

The sampling image containing the cortical contours was used to establish the location of transverse lines (Fig. 3D). In Northern Eclipse, equidistant (131µm) points are automatically generated along a center orienting line (i.e. the manually traced layer IV). For each point, the software constructs a transverse line which passes through the point, traverses the shortest distance between the inner and outer contour while minimizing the deviation from 90 degrees on the angle with the center orienting line and does not cross any other transverse line. The pixel values underlying each transverse line are sampled serially from the outer to the inner contour and exported as a column of values to Excel. The same grill of transverse lines is used to sample each of the other six equally sized sampling images so that the sample from any one transverse corresponds to the same location on each of the images. In R (the shareware version of S-plus, a statistics software environment), each transverse sample representing a profile of the cortex was resampled by linear interpolation to a common length for the purpose of comparison (i.e. the profile values from the outer to the inner contour of the cortex were transformed to a scale of 0-100% depth). The depth of the individual cortical layers on each profile was identified from the sample of the images containing the traced location of the cortical layers (Fig. 4C-F, 5). An estimate of the density of the cortical layers was then obtained by calculating the average value on each profile of a limited neighborhood of values around the identified depth of the respective cortical layer (Fig. 5). In order to pool data across sections of different thickness, the estimated laminar densities were standardized against the mean density of the entire profile. The standardized laminar features were grouped according to architectonic area. Further statistical analyses were performed in Statistica. The profile features were z-transformed on a hemisphere by hemisphere basis.

3.5 Cortical Folding and Spatially Overlapping Neuronal Layers

Cortical folding modulates the relative depth of the cortical layers such that, when the cortex is concave, the inner neuronal layers are thinner relative to the outer layers and, when the cortex is convex, the converse relation obtains between the inner and outer layers (Bok, 1959; Hilgetag & Barbas, 2006). To determine whether our measurements were affected by morphological position we compared the features of interest with a measure of cortical curvature, namely the relative depth of layer IV. The granule density of layer IV and pyramidal density of layer Va were only minimally correlated with cortical curvature r = -0.06 and 0.23, respectively. Another methodological concern was the proximity of the layers IV and Va which could interfere with the estimation of their individual contributions to the density profile. The density of layers IV and Va estimated on profiles sampled from the general density images were highly correlated, r = 0.82 in contradiction with observable architectonic variation on the histological sections. The successful segregation of the cortical layers on the basis of typical neuron size, i.e the selection of layers II and IV in the granule cell density images and the selection of layers III, V and VI in the pyramidal cell density images (Fig. 3B,C), was indicated by the low correlation, r = -0.12 between the densities of layer IV and Va sampled, respectively, on the granule and pyramidal cell density images. An investigation of the influence of these and other sampling parameters on the data are reported in Mackey & Petrides (2009).

4. Results

The location of architectonically comparable areas in the orbital and ventromedial frontal cortex of the human and the macaque brains is shown in Figure 6. Figure 7A,B illustrates the close match in the mean quantified densities of layers IV and Va between comparable areas in the human and the macaque brains. The mean laminar densities per area were rank ordered separately in the two species. A statistical comparison of the area rankings demonstrated that the architectonic match between comparable areas is significant (Spearman rank test, layer IV: r = 0.976 and layer V: r =0.988; p<0.00001). For quick reference, the key criteria which distinguish between neighboring architectonic areas are listed in Tables 1 and 2. Area 25 in the posterior-most region of the ventromedial surface of the frontal lobe and extending a short distance onto the orbital surface and area 24, found along the margin of the corpus callosum (Fig. 1 and 6), lack a granule layer IV and present a simple arrangement of pyramidal layers with a notably dense layer V. Because both areas are agranular (i.e. lack a granule layer IV) and have an equally dense layer V, they are grouped together in the quantitative data, although several other visible criteria distinguish them (e.g. area 24 has a less dense layer VI). Area 32, which exhibits an emergent though still faint layer IV (i.e. this cortex is dysgranular), forms a buffer between these latter simple agranular areas and the more anteriorly placed granular area 14 medial (14m). From areas 24/25 through area 32 to area 14m, there is a marked increase in laminar complexity, such that sublamination of the pyramidal layers, III V and VI becomes increasingly obvious. Along the medial orbital surface which includes the gyrus rectus and the medial orbital gyrus (Fig. 1), from the posterior area 25 toward the frontal pole, there is a progressive increase in the density of granule layer IV and a decrease in the density of pyramidal layer Va that is divided into a series of steps labeled 14 caudal (14c), 14 rostral (14r), and 11 medial (11m). Area 14c is almost agranular and contains a prominent layer Va. In dysgranular area 14r, the prominence of layer Va decreases vis-à-vis the density of the other pyramidal layers and decreases yet again anteriorly in granular area 11m. Like the ventromedial cortex, the sublamination of the pyramidal layers on the medial orbital surface becomes more evident from posterior to anterior. It is notable that all areas in the ventromedial and the medial orbital regions, areas 24, 25, 32 and all parts of area 14, share a dense layer Va feature. Moving lateral onto the central and posterior part of the orbital surface that is labeled as area 13, the dense layer Va of area 14 is replaced by a diffusely arranged collection of pyramidal neurons and the granule cell layer IV is poorly defined. Anterior to area 13 is a granular cortical area located on the anterior orbital gyrus of both species (Fig 1 and 6), area 11, which in contrast to area 13 possesses more clearly arranged sublaminations of the inner layers V and VI (Fig 2B). This trend of increasing laminar complexity in the posterior to anterior direction is continued on the lateral orbital gyrus (Fig. 1) where two parts of area 47/12 were identified, 47/12 orbital (14/12o) and 47/12 medial (47/12m). Area 47/12m is more granular and more clearly sublaminated than its posterior neighbor area 47/12o. These latter two areas are set apart from the more medial cortical areas by the presence of large pyramidal cells in the deep part of layer III and a relatively less dense layer Va. Separate ANOVAs on the human and macaque samples revealed a significant overall difference between areas (human: $F(18, 128\ 454) = 856.19$, $p<0.0001$; macaque: $F(18, 19450) = 167.34$, $p<0.0001$). Further analysis by Tukey's HSD post hoc tests demonstrated significant differences between all adjacent areas in the human brain (and most adjacent areas in the monkey brain) on at least one of the measured features, $p<0.01$. In the monkey, the differences between paired adjacent areas 32 and 14c, 14r and 11m, and 11m and 11 failed to reach significance (Fig. 6) although in each of these cases the direction of the change in density between areas matched that found between comparable areas of the human cortex (Fig. 7). To determine whether the pattern of results was stable in both hemispheres, the data were also coded as right or left hemisphere and the means compared by cross-factorial ANOVA which again indicated a difference between areas (human: $F(18, 224) = 30.46$, $p<0.0001$ monkey: $F(18, 88) = 11.47$, $p<0.0001$) but no significant difference between hemispheres or interaction effect.

In addition to identifying specific architectonically comparable areas in the two species, the overall ordering of the mean quantified densities of layers IV and Va arrange the areas of interest along two dimensions which mirror their spatial position within the total constellation of areas (Fig 7A, B). First, there is a medial to lateral decrease in the density of layer Va and, second, there is a posterior to anterior increase in the density of layer IV.

5. Discussion

More than seventy-three thousand areal density profiles were collected from 16 human and 7 macaque post-mortem hemispheres. Two features estimated from the profiles, the densities of layers IV and Va, were of primary interest for several reasons. Unlike abstract mathematical features, such as central moments (Schleicher *et al.*, 2005) derived from areal density profiles in previous within species studies, sampled layer IV and Va densities clearly correspond to unique visible phenomena in the histological specimen. Consequently, these features are directly comparable to observations in the existing qualitative architectonic literature. Since the qualitative descriptions of the macaque frontal cortical architecture are highly consistent (Walker, 1940; Morecraft, Geula & Mesulman, 1992; Barbas & Pandya, 1989; Carmichael & Price, 1994; Petrides & Pandya, 1994), the standard labeling of areas in the macaque served as an uncontroversial template for the labeling of areas with similar quantitatively sampled architectonic features in the human brain. The densities of layers IV and Va also figured prominently in our own visual observations and we were able to distinguish all architectonic areas reported here from their neighbors on the basis of one or both of these features. These features also have known biological significance (e.g. layer IV neurons are the target of projections from the thalamus and layer V neurons project to several subcortical structures) (Negyessy & Goldman-Rakic, 2005; Zikopoulos & Barbas, 2006) which, in turn, may facilitate the integration of our data with emerging theories on the unique computational contributions of particular cortical layers (Brown, Bullock & Grossberg, 2004). Layer IV and Va densities have also been explicitly cited in hypotheses on the progressive differentiation of the cortex (Sanides 1964; Barbas & Pandya, 1989) which we explore here in human specimens. Most importantly, these two architectonic features are unambiguously comparable between the human and the macaque brains.

The prominence of layer Va in medial areas 25, 24, 32, and 14 in contrast to the less dense layer Va found in the central and lateral orbital areas 13, 11, and 47/12 (Fig. 7B) suggests an architectonic grouping of areas consistent with tract tracing studies in the macaque which indicate the existence of two separate highly interconnected networks of areas that possess distinct patterns of connectivity with the rest of the brain (Price, 2007; Barbas, 2007). In the macaque, the *orbital network*, areas 13, 11 and 47/12, receives projections from olfactory, gustatory, visual and somatosensory cortex and has been implicated in the rapid flexible coding of rewarding stimuli (Murray, O'Doherty & Schoenbaum, 2007). Since these cortico-cortical connections are bi-directional, the orbital network is well placed to bias the activity and perhaps reorganize the processing of sensory systems towards currently rewarding stimuli. The *medial network* (which also includes the medial orbital region), areas 25, 24, 32 and 14, is connected bi-directionally most heavily with non-sensory brain structures such as the amygdala, hippocampus and hypothalamus and thus is appropriately positioned to mediate the relation of memory with the regulation of the internal milieu (Damasio, 1996). Probabilistic patterns of connectivity similar to those described for the medial and orbital networks in the macaque have been found in the human brain by in vivo neuroimaging on the basis of a morphological parcellation of the ventromedial and orbital frontal cortex which resembles and, thus, in part, confirms the present identification of architectonically comparable areas in the two species (Croxson *et al.,* 2005).

The second identified dimension of architectonic variation is a posterior to anterior increase of layer IV density (Fig. 4A) i.e. from the absence of layer IV (agranular areas 24 and 25 and almost agranular area 14c) to its emergence (dysgranular areas 32, 13, 14r, and 12o) and continued development (granular areas 11, 11m, 12m, and 14m), which we have grouped as: posterior, intermediate and anterior, noting that intermediate areas 13 and 12o are bordered posteriorly by agranular cortex (Walker, 1940; Morecraft, Geula & Mesulam, 1992; Barbas & Pandya, 1989; Carmichael & Price, 1994; Petrides & Pandya, 1994) extending from the insular region. The increase in layer IV density is accompanied by greater laminar complexity which has been shown by tract tracing studies in the monkey to predict the distribution of inter-area connectivity in the frontal cortex (Barbas, 2007). Frontal areas with greater laminar differentiation receive input to layer I from the infragranular layers V and VI of areas with less laminar differentiation and return information to these latter areas by a projection to layers V and VI (Barbas, 1986; Barbas and Rempel-Clower, 1997). The pattern of laminar inputs and outputs in the frontal cortex has been likened to the feed-forward and feed-back pathways found in the visual, auditory and somatosensory streams which indicate a direction or hierarchy in the flow of information from basic to more abstract processing stages (Shipp, 2005). Here, we indicate the location of a similarly organized flow of information between networks of comparable architectonic areas in the ventral frontal cortex of the human brain. Considering also the complete or almost complete absence of granule layer IV in the frontal lobe of non-primate species (Jelsing *et al.,* 2006), the elaboration of the cortex towards the frontal pole suggests the possibility of a hierarchy of areas (posterior to anterior dimension) in both the medial and orbital networks (medial to lateral dimension) where the structurally complex anterior granular cortex is recruited in the performance of more specialized emotional acts within the primate behavioral phenotype.

6. Figures, and Legends

Table 1 (Changes in density of layer IV between neighboring areas)

Areas										
24/25	------	< 32	------	< 14c	------	------	------	------	------	------
32	> 24/25	------	< 14m	> 14c	------	------	------	------	------	------
14m	------	> 32	------	> 14c	> 14r	> 11m	------	------	------	------
14c	------	< 32	< 14m	------	< 14r	------	------	< 13	------	------
14r	------	------	< 14m	> 14c	------	< 11m	< 11	= 13	------	------
11m	------	------	< 14m	------	> 14r	------	< 11	------	------	------
11	------	------	------	------	> 14r	> 11m	------	> 13	------	= 12m
13	------	------	------	> 14c	= 14r	------	< 11	------	< 12o	< 12m
12o	------	------	------	------	------	------	------	> 13	------	< 12m
12m	------	------	------	------	------	------	= 11	> 13	>12o	------

Table 2 (Changes in density of layer Va between neighboring areas)

areas										
24/25	------	= 32	------	= 14c	------	------	------	------	------	------
32	= 24/25	------	= 14m	= 14c	------	------	------	------	------	------
14m	------	= 32	------	= 14c	> 14r	> 11m	------	------	------	------
14c	= 24/25	= 32	= 14m	------	> 14r	------	------	> 13	------	------
14r	------	------	< 14m	< 14c	------	> 11m	> 11	> 13	------	------
11m	------	------	<14m	------	< 14r	------	> 11	------	------	------
11	------	------	------	------	< 14r	< 11m	------	> 13	------	> 12m
13	------	------	------	< 14c	< 14r	------	< 11	------	> 12o	> 12m
12o	------	------	------	------	------	------	------	< 13	------	< 12m
12m	------	------	------	------	------	------	< 11	< 13	> 12o	------

Tables 1 and 2 present the key architectonic changes which we observed qualitatively between each area (1st column) and its immediate neighbors in terms of layer IV and layer Va density, respectively. Every area could be differentiated visually from each of its neighbors according to changes in one or both of these architectonic features.

Figure 1

Morphology of the ventromedial (A and C) and orbital (B and D) surfaces of the human and monkey frontal cortex respectively. The conventional orientations of the brain are indicated (synonymous orientations are noted in brackets). Sulci and gyri are labeled in white and red, respectively. Note that the labeling of the superior rostral sulcus (SRS) and the inferior rostral sulcus (IRS) on the ventromedial surface follows the nomenclature established in previous architectonic studies (Vogt *et al.*, 1995; Economo & Koskinas, 1925). In studies based on morphology alone (Paus, 1996; Fornito *et al.,* 2006) the term *superior rostral sulcus* labels the first major horizontal sulcus (denoted by *) ventral to the corpus callosum (CC). Abbreviations: AOG, anterior orbital gyrus; APS, anterior parolfactory sulcus; CG, cingulate gyrus; GR, gyrus rectus; HR, horizontal ramus of the sylvian fissure; IMG, inferior medial gyrus; LOG, lateral orbital gyrus; LOS, lateral orbital sulcus; MOG, medial orbital gyrus; MOS, medial orbital sulcus; MPS, medial polar sulci; OLFS, olfactory sulcus; OLFg, olfactory groove; POG, posterior orbital gyrus; RS, rostral sulcus; SMG, superior medial gyrus; TOS, transverse orbital sulcus.

Figure 2

A.Various parts of the orbital frontal cortex designated by different investigators as an area which would be comparable architectonically to monkey area 13: vertical bars (Petrides & Mackey, 2005), circles (Hof, Mufson & Morrison, 1995), horizontal bars

(Ongur, Ferry & Price, 2003) triangles (Semendeferi *et al.*, 1998). Major gyri are labeled as in Figure 1. B. Digital photomicrographs of the cortical architecture in the central orbital region, areas 13 and 11 as determined by the present quantitative investigation (Fig. 3), in the human and the macaque brains. Cortical layers are identified by Roman numerals. The inner and outer boundaries of layer IV which is composed of small round granule neurons is labeled in each photograph by curved black lines. The bar in the lower right corner represents 200µm. In both species, area 13 is a dysgranular cortex (i.e. layer IV is poorly organized and lightly populated with granule cells) with diffusely arranged pyramidal cells in layers V and VI, while area 11 is an example of granular cortex (i.e. layer IV is clearly organized and well populated) with a more clearly defined sublamination of the inner layers V and VI.

Figure 3

Illustration of the (A) general, (B) granule and (C) pyramidal cell density images. Shades of grey approaching white indicate higher neuronal density. Note that, in the granule cell density image, there are two bands of higher neuronal concentration which correspond to granule cell layers II and IV. In the pyramidal cell density image, there are three bands of higher neuronal concentration which correspond to pyramidal layers III, V and VI. D. Illustration of transverse lines which span the width of the cortex. The pixel values underlying each transverse line are sampled serially from the outer to the inner contour and represent a profile of neuronal density at that location. This same set of transverse lines is then used to sample 7 equally sized images which contain different information about the cortical lamina (A-C and Supplementary Fig. C-F).

Figure 4

Illustration of the traced neuronal layers II, IV, Va and VIa as well as the inner and outer contour of the cortex. A. Example image of the cortex. Note the resolution has been reduced for publication. B. Illustration of manually identified neuronal layers II, IV, Va and VIa as well as the inner and outer contours of the cortex. Layer II is located by drawing a line along its inner boundary with layer III, while layers IV, Va and VIa are identified by tracing a line through the center of each of these layers. Everything outside layer II and outside the brain on the image is masked in white (outer contour) and everything inside layer VI, i.e. the white matter, is masked in black (inner contour). C-F Illustrate the four equally sized images that are then generated from the manually traced layers.

Figure 5

Example of a density profile sampled from a granule cell density image in order to illustrate how the density of layer IV is estimated. Alternating background blocks of light and dark brown identify the neuronal layers which are labeled by roman numerals along the top of the figure. The granule cell density profile and is plotted as a black line in the top half of the illustration. The profile was sampled from the part of the granule cell density image displayed in the bottom half of the figure. Also shown is the part of the thresholded image from which the granule cell density images was derived. Note the small round granule cell neurons in layers II and IV. Along the horizontal center of the figure, the cortical depth is indicated in percent. Above this axis, a long dark brown line denotes the region on the profiles used to calculate the mean density of the profile (from the inner boundary of layer II to layer VIa). Above the long brown line is a short brown line that indicates the region on the profile defined as representative of layer IV. A circle in the center of the short line marks the location of layer IV as coded in the profile sampled from the image containing the manually traced neuronal layer IV (e.g. Supplementary Fig. 1D).

Figure 6

Architectonic parcellation of the human and monkey orbital and ventromedial surface. Comparable areas between species share the same number label and are identified also by matching colors.

Figure 7

Matching mean density of layer IV (A) and layer Va (B) between comparable architectonic areas in the monkey (dark blue) and the human (light blue) brains. Error bars indicate standard deviation. A. Architectonic areas are ordered along the x-axis by increasing layer IV density in the monkey. Ordering by the mean density of layer IV arranges areas into groups that mirror their morphological position in a posterior to anterior direction. The range of the spatial groupings: posterior, intermediate and anterior, are indicated by a funnel symbol underneath the relevant architectonic areas. B. Architectonic areas are ordered along the x-axis by decreasing layer Va density in the monkey. Ordering by the mean density of layer Va arranges areas into groups that coincide with their morphological position in a medial to lateral direction. The range of the spatial groupings: ventromedial, medial orbital, central orbital, and lateral orbital are indicated by a funnel symbol underneath the relevant areas.

7. References

Barbas, H. & Pandya, D. (1989) Architecture and intrinsic connections of the prefrontal cortex in the rhesus monkey. *J. Comp. Neurol.,* **286**, 353-375.

Barbas, H. (2007) Specialized elements of orbitofrontal cortex in primates. *Ann. N. Y. Acad. Sci.,* **1121**, 10-32.

Beck, E. (2009) A cytoarchitectural investigation into the boundaries of cortical areas 13 and 14 in the human brain. *J. Anat.,* **83**, 147-157.

Blair, R. (2004) The roles of orbital frontal cortex in the modulation of antisocial behavior. *Brain and Cognition*, **55**, 198-208.

Bok, S. (1959) *Histonomy of the Cerebral Cortex*. Elsevier, New York.

Brown, J., Bullock, D., & Grossberg, S. (2004) How laminar frontal cortex and basal circuits interact to control planned and reactive saccades. *Neural Networks,* **17**, 471-510.

Carmichael, S. & Price, J. (1994) Architectonic subdivision of the orbital and medial prefrontal cortex in the macaque monkey. *J. Comp. Neurol.* **346**, 366-402.

Cavada, C., Company, T., Tejedor, J., Cruz-Rizzolo, R. J., & Reinoso-Suarez, F. (2000) The anatomical connections of the macaque monkey orbitofrontal cortex. A review. *Cereb. Cortex,* **10**, 220-242.

Croxson, P., Johansen-Berg, H., Behrens, T., Robson, M., Pinsk, M., Gross, C., Richter, W., Richter, M., Kastner, S., & Rushworth, M. (2005) Quantitative investigation of connection of the prefrontal cortex in the human and macaque using probabilistic diffusion tractography. *J. Neurosci.,* **25**, 8854-8866.

Damasio, A. (1996) The somatic marker hypothesis and the possible functions of the prefrontal cortex. *Phil. Trans. R. Soc. Lond. B,* **351,** 1413-1420.

Dombrowski, S., Hilgetag, C., & Barbas, H. (2001) Quantitative architecture distinguishes prefrontal cortical systems in the rhesus monkey. *Cereb. Cortex,* **11,** 975-988.

Economo, C. (1929) *The cytoarchitectonics of the human cerebral cortex.* Parker, S. (trans), Oxford University Press, London.

Everitt, B., Hutcheson, D., Ersche, K., Pelloux, Y., Dalley, J., & Robbins, T. (2007) The orbital prefrontal cortex and drug addiction in laboratory animals and humans. *Ann. N. Y. Acad. Sci.,* **1121,** 576-597.

Fornito, A., Whittle, S., Wood, S., Velakoulis, D., Pantelis, C., & Yucel, M. (2006) The influence of sulcal variability on morphometry of the human anterior cingulate and paracingulate cortex. *Neuroimage,* **33,** 843-854.

Goldstein, J., Goodman, J., Seidman, L., Kennedy, D., Makris, N., Lee, H., Tourville, J., Caviness, V., Faraone, S., & Tsuang, M. (1999) Cortical abnormalities in schizophrenia identified by structural magnetic resonance imaging. *Arch. Gen. Psychiatry,* **56**, 537-547.

Harlow, J. (1848/1999) Passage of an iron rod through the head. *J. Neuropsychiatry Clin. Neurosci.,* **11**, 281-283.

Hilgetag, C. & Barbas, H. (2006) Role of mechanical factors in the morphology of the primate cerebral cortex. *PLoS Comput. Biol.* **2(3)** e22.

Hof, P., Mufson, E., & Morrison, J. (1995) Human orbitofrontal cortex: cytoarchitecture and quantitative immunohistochemical parcellation. *J. Comp. Neurol.,* **359**, 48-68.

Jelsing, J., Hay-Schmidt, A., Dyrby, T., Hemmingsen, R., Uylings, H., & Pakkenberg, B. (2006) The prefrontal cortex in the Gottingen minipig brain defined by neural projection criteria and cytoarchitecture. *Brain Res. Bull.,* **70**, 322-336.

Kringelbach, M. & Rolls, E. (2004) The functional neuroanatomy of the human orbitofrontal cortex: evidence from neuroimaging and neuropsychology. *Progress in Neurobiology,* **72**, 341-372.

Mackey, S. & Petrides, M. (2009) Architectonic mapping of the medial region of the human orbitofrontal cortex by density profiles. *Neurosci*. **159**, 1089-1107.

Morecraft, R., Geula, C., & Mesulam, M-M. (1992) Cytoarchitecture and neural afferents of orbitofrontal cortex in the brain of the monkey. *J. Comp. Neurol.* **323**, 341-358.

Murray, E., O'Doherty, J., & Schoenbaum, G. (2007) What we know and do not know about the functions of the orbitofrontal cortex after 20 years of cross-species studies. *J. Neurosci*., **27**, 8166-8169.

Negtessy, L. & Goldman-Rakic, P. (2005) Morphometric characterization of synapses in the primate prefrontal cortex formed by afferents from the mediodorsal thalamic nucleus. *Exp. Brain Res.* 1**64**, 148-154.

Ongur D, Ferry A, & Price J. (2003) Architectonic subdivision of the human orbital and medial prefrontal cortex. *J. Comp. Neurol.* **460**, 425-449.

Petrides, M. & Mackey, S. (2006) The orbitofrontal cortex: sulcal and gyral morphology and architecture. In Zald, D. & Rauch, S. (eds), *The Orbitofrontal Cortex.* Oxford University Press, Oxford, pp. 19-37.

Phelps, E., Delgado, M., Nearling, K., & LeDoux, J. (2004) Extinction learning in humans: role of the amygdala and vmPFC. *Neuron*, **16**, 897-905.

Price, J. (2007) Definition of the orbital cortex in relation to specific connections with limbic and visceral structures and other cortical regions. *Ann. N. Y. Acad. Sci.,* **1121**, 54-71.

Ressler, K. & Mayberg, H. (2007) Targeting abnormal neural circuits in mood and anxiety disorders: from the laboratory to the clinic. *Nat. Neurosci*. **10**, 1116-1124.

Sanides, F. (1964) The cyto-myeloarchitecture of the human frontal lobe and its relation to phylogenetic differentiation of the cerebral cortex. *Journal fuer Hirnforschung* 269-282.

Schleicher, A., Palomero-Gallagher, N., Morosan, P., Eickhoff, S., Kowalski, T., de Vos. K,, Amunts, K., & Zilles, K. (2005) Quantitative architectural analysis: a new approach to cortical mapping. *Anat. Embryol.,* **210**, 373-386.

Semendeferi, K., Armstrong, E., Schleicher, A., Zilles, K., & Van Hoesen, G. (1998) Limbic frontal cortex in hominoids: a comparative study of area 13. *Am. J. Phys. Anthropol.* **106**, 129-155.

Vogt, B., Nimchinsky, E., Vogt, L., & Hof, P. (1995) Human cingulate cortex: surface features, flat maps, and cytoarchitecture. *J. Comp. Neurol.* **359**, 490-506.

Walker, A. (1940) A cytoarchitectural study of the pre-frontal area of the macaque monkey. *J. Comp. Neurol.* **73**, 59-86.

Zikopoulos, B. & Barbas, H. (2006) Prefrontal projections to the thalamic reticular nucleus form a unique circuit for attentional mechanisms. *J. Neurosci.* **26**, 7348-7361.

Figure 1 Chapter 3

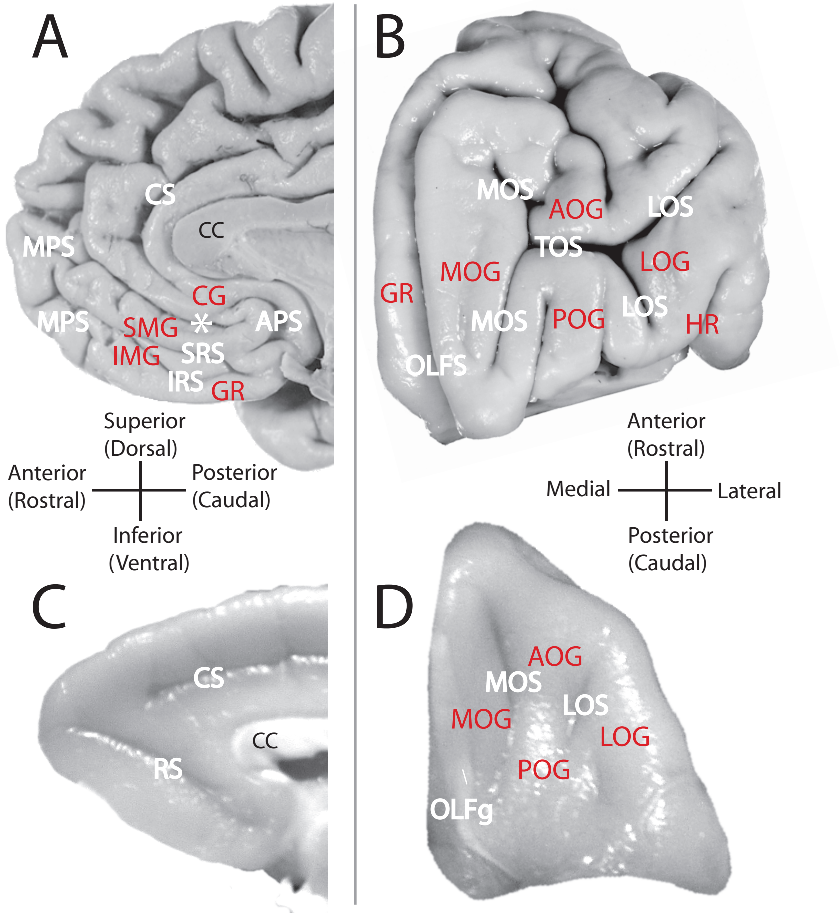

Figure 2 Chapter 3

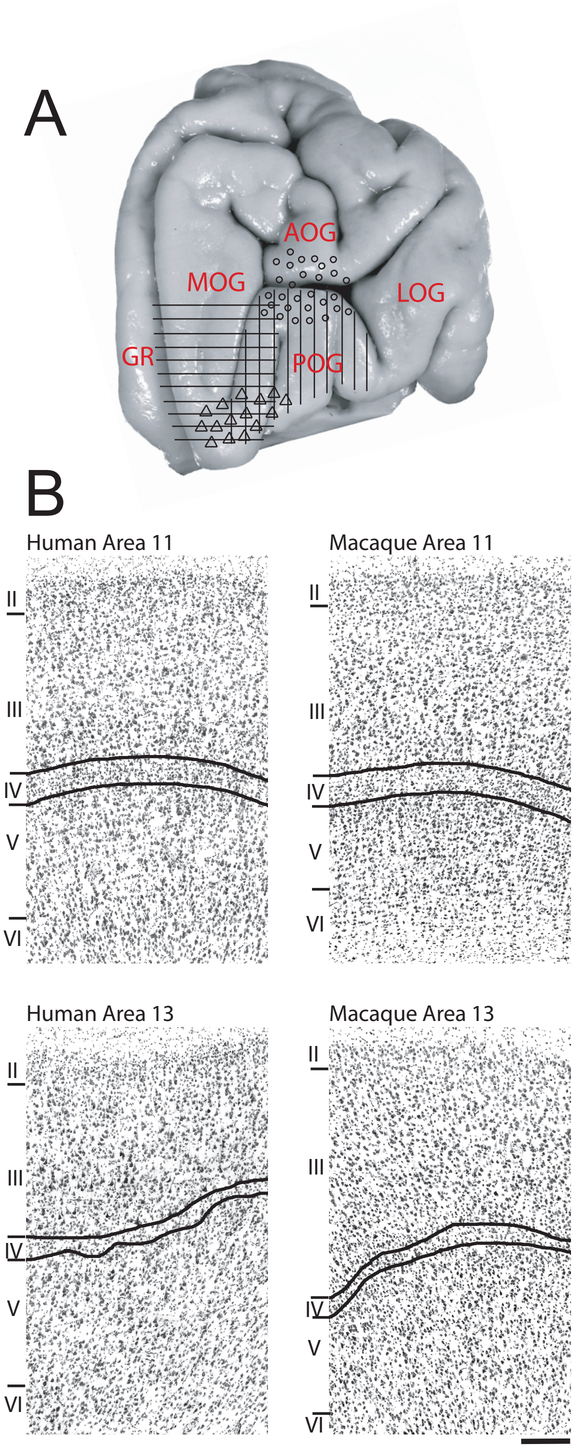

Figure 3 Chapter 3

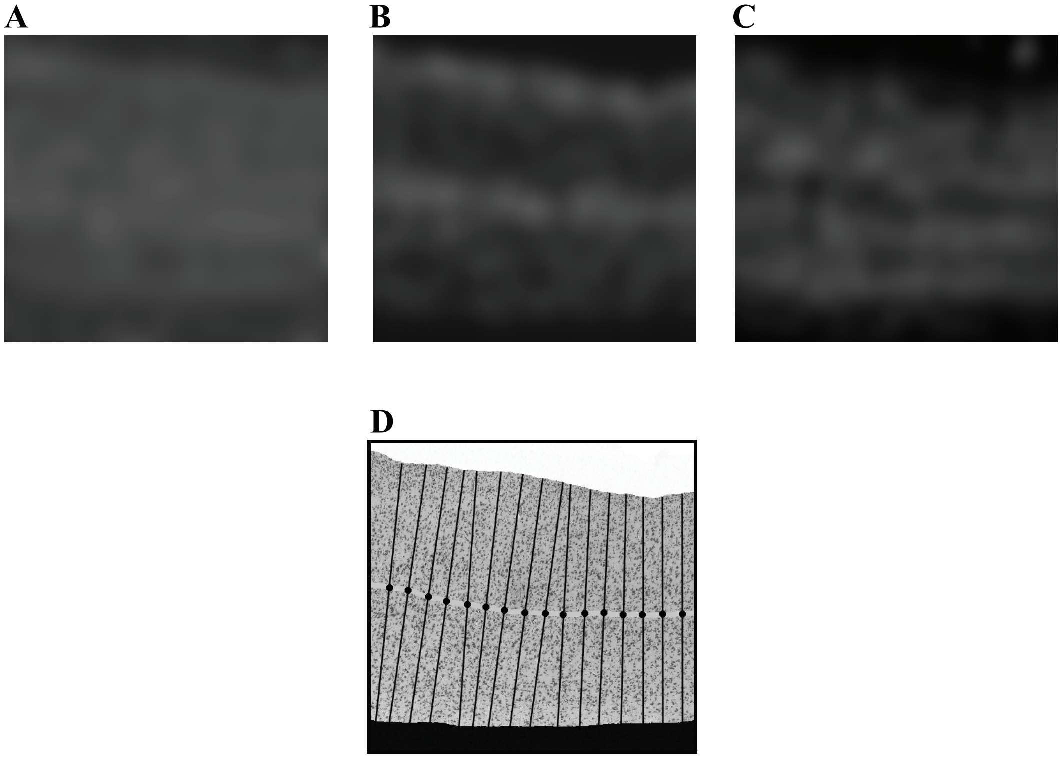

Figure 4 Chapter 3

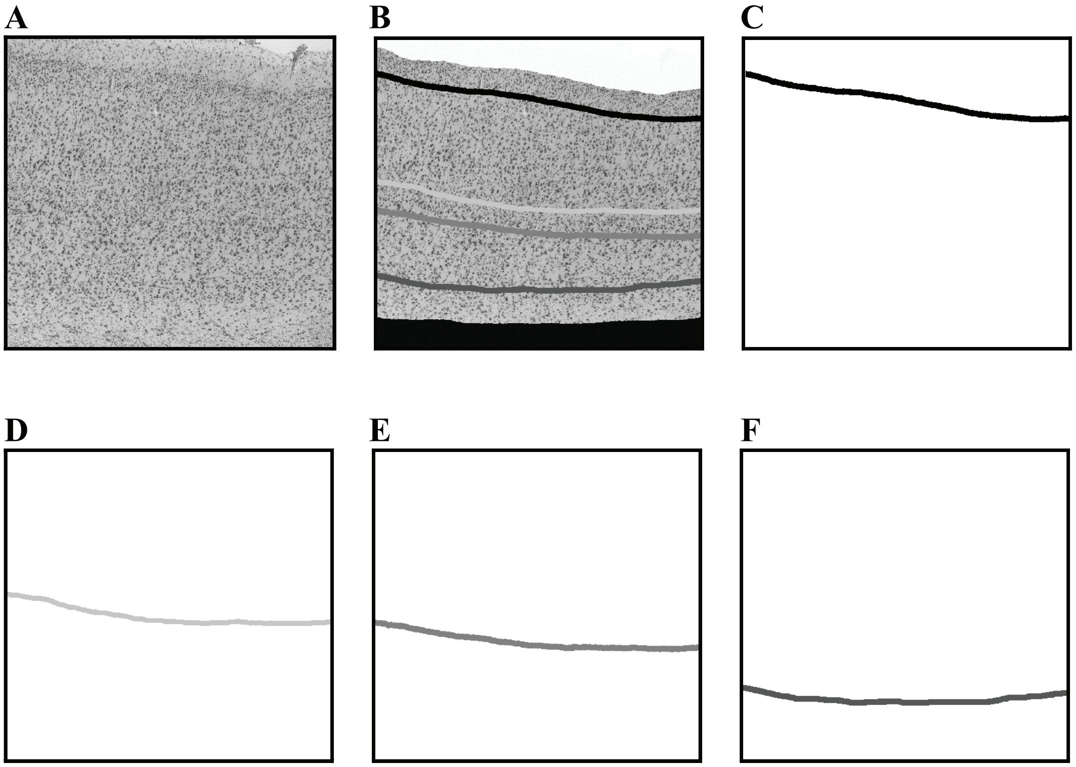

Figure 5 Chapter 3

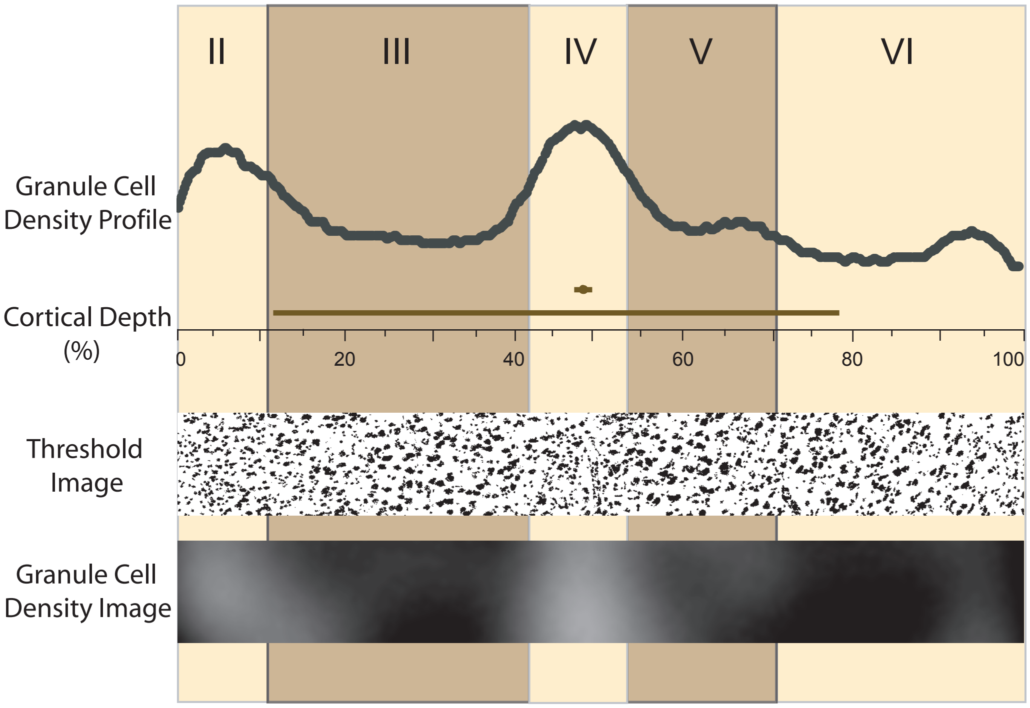

Figure 6 Chapter 3

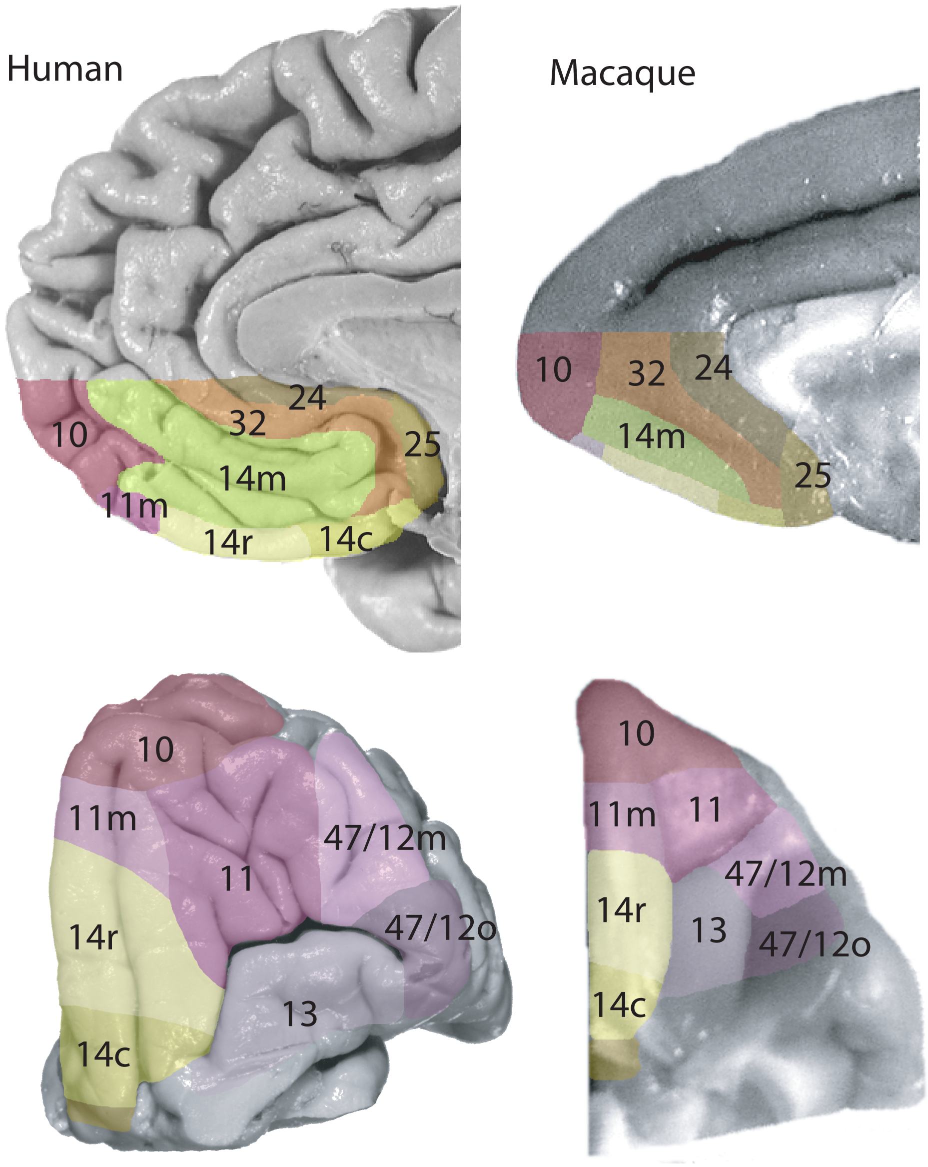

Figure 7 Chapter 3